PHYSICAL REVIEW C VOLUME 59, NUMBER 1 JANUARY 1999

Calculations of reaction cross sections for ^{19}C at relativistic energies

J. A. Tostevin and J. S. Al-Khalili
Department of Physics, School of Physical Sciences, University of Surrey, Guildford, Surrey, GU2 5XH, United Kingdom
(Received 9 October 1998)

Few-body Glauber theory calculations of reaction cross sections for the proposed single neutron halo nucleus ^{19}C are presented for an incident energy of 960 MeV/nucleon on a ^{12}C target. The calculated reaction cross sections are shown to be significantly smaller than those obtained using the optical limit approximation to the Glauber theory elastic profile function. The implications of these differences upon the deduced size and structure of the extended ^{19}C ground state, from newly reported interaction cross-section measurements, are discussed, including the sensitivity of the cross sections to the assumed ^{19}C single neutron separation energy. [S0556-2813(99)50101-5]

PACS number(s): 21.10.Gv, 11.80.Fv, 25.10.+s, 27.20.+n

There is now a history of the use of interaction cross-section measurements, at energies of several hundred MeV/nucleon, to estimate the sizes and matter distributions of exotic nuclei produced in high-energy fragmentation reactions [1–3]. Until quite recently, the optical limit (OL) approximation to Glauber theory [4–6] has been used as the theoretical basis of such analyses. The inputs to this approximate description are the projectile and target nucleus one-body densities whose geometric overlap at a given impact parameter, when multiplied by the appropriate nucleon-nucleon (NN) reaction cross section, determines the projectile-target total reaction cross section. This cross section is then compared with measurements. This approach was shown to work well for normal, spatially localized, nuclei in which the nucleons occupy a well-defined mean field volume [7].

The most dramatic feature of halo nuclei, however, is their very loosely bound few-body character, with a strong spatial localization of the core nucleons and a delocalization of the halo particles. More recent theoretical analyses have shown that an explicit treatment of this correlated few-body nature, or granularity, is important quantitatively for calculations of reaction cross sections [8–11]. Such a few-body description leads to smaller calculated reaction cross sections than are obtained from the OL approximation with significant implications for the deduced size and ground state structure of the halo [9]. It follows that interaction cross-section analyses, even of high energy data, are model dependent and require the use of theoretical relative motion wave functions for these few-body structures, e.g. [9,11].

In this Rapid Communication, we examine the importance of these few-body effects for the nucleus ^{19}C. This, the last particle-stable odd-neutron isotope of carbon, is suggested to be a single neutron halo nucleus [12,13] with a neutron separation energy $S_n \approx 240 \pm 100$ keV, although this value is a world average of several experiments each with significant uncertainties [13,14]. New interaction cross-section measurements have recently been reported [15] for ^{19}C, and for its core ^{18}C, on a ^{12}C target at energies of 960 and 955 MeV/nucleon, respectively. The data were accompanied by an analysis using the optical limit approximation. The conclusion drawn was that the ^{19}C datum is consistent with a halo ground state of ^{19}C, but with a 46% $(0^+ \otimes 2s_{1/2})$ ^{18}C ground state and a 54% $(2^+ \otimes 1d_{5/2})$ ^{18}C $(2^+;$ 1.62 MeV) excited core state admixture. We reexamine this result in the light of the calculated few-body model cross sections.

The reaction cross section of projectile P and target T at high energy is written [4]

$$\sigma_R(P) = 2\pi \int_0^\infty dbb[1 - |\mathcal{S}_P(b)|^2], \tag{1}$$

involving the squared modulus of the elastic profile function $\mathcal{S}_P$ for the P-T system at a collision impact parameter b. In the optical limit approximation to Glauber theory,

$$\mathcal{S}_P^{OL}(b) = \exp\left(-\frac{\overline{\sigma}_{NN}^{PT}}{2} \int d^2\mathbf{x} \rho_P^{(z)}(|\mathbf{x}|) \rho_T^{(z)}(|\mathbf{b}-\mathbf{x}|) \right), \tag{2}$$

where $\overline{\sigma}_{NN}^{PT}$ is the isospin averaged NN cross section appropriate for the given P-T combination. The nuclear ground state matter distributions ρ_P and ρ_T enter here as (z-integrated) thickness functions $\rho_i^{(z)}(b)$ $(i = P,T)$, e.g. [9], with the z axis in the beam direction.

Of particular interest here are one neutron-halo projectiles, strongly clustered two-body systems of a neutron and a core $(n+C)$. It is then the constituent neutron- and core-target two-body systems which have the localized nature appropriate for the use of the optical limit approximation. As has been discussed fully elsewhere [4,9,16], the few-body (FB) elastic profile function is

$$\mathcal{S}_P^{FB}(b) = \langle \Phi_0 | \mathcal{S}_C^{OL}(b_C) \mathcal{S}_n^{OL}(b_n) | \Phi_0 \rangle, \tag{3}$$

where Φ_0 is the ground state relative motion wave function of the neutron and core. The bra-ket denotes integration over the projectile internal coordinates. Here the core-target OL profile function is given by Eq. (2), but in terms of the core density ρ_C, while for the neutron

$$\mathcal{S}_n^{OL}(b_n) = \exp\left(-\frac{\overline{\sigma}_{NN}^{nT}}{2} \rho_T^{(z)}(b_n) \right). \tag{4}$$

We calculate FB cross sections for the one-neutron halo nucleus ^{19}C. To make comparison with OL calculations, we also construct the $(A=19)$ projectile one-body density $\rho_P(r) = \hat{\rho}_C(r) + \hat{\rho}_n(r)$, where

$$\hat{\rho}_C(r)=\int d^3\mathbf{x}\rho_C(|\mathbf{r}-\mathbf{x}|)\rho_{cm}(\mathbf{x}),\ \ \rho_{cm}(\mathbf{x})=A^3|\Phi_0(A\mathbf{x})|^2, \tag{5}$$

and

$$\hat{\rho}_n(\mathbf{r})=\left(\frac{A}{A-1}\right)^3\left|\Phi_0\left(\frac{A}{A-1}\mathbf{r}\right)\right|^2. \tag{6}$$

More details can be found in [9]. In common with previous analyses of experimental data, we calculate reaction cross sections σ_R and make comparison with the experimental interaction cross sections σ_I, a procedure expected to be accurate for halo nuclei [16].

We calculate, in OL approximation, the profile functions $\mathcal{S}_{18}^{OL}$ and $\mathcal{S}_n^{OL}$ for the ^{18}C- and neutron-^{12}C subsystems, and also their reaction cross sections $\sigma_R^{OL}(^{18}\mathrm{C})$ and $\sigma_R^{OL}(n)$. For comparison with the earlier OL analysis [15], we also calculate the composite (halo) nucleus cross section $\sigma_R^{OL}(^{19}\mathrm{C})$. In all calculations, we use the free NN cross sections parameterized by Charagi and Gupta [17]. For the isospin zero ^{12}C target, the required isospin averaged $\overline{\sigma}_{NN}$ are 44.058 mb and 44.145 mb at 955 and 960 MeV, respectively. A Gaussian matter distribution is assumed for the ^{12}C target with an rms matter radius $\langle r^2\rangle_{12}^{1/2}=2.32$ fm [3]. With these inputs, assuming also a Gaussian matter distribution for the ^{18}C, we obtain a core rms radius $\langle r^2\rangle_{18}^{1/2}=2.70\pm0.04$ fm, which generates a $\sigma_R^{OL}(^{18}\mathrm{C})=1103.4$ mb at 955 MeV/nucleon. The empirical datum is 1104 ± 15 mb [15]. We attribute the small difference between our deduced $\langle r^2\rangle_{18}^{1/2}$ and that of [15] to the choice of effective NN cross sections used, which are not stated in [15]. The calculated neutron-^{12}C cross section at 960 MeV, $\sigma_R^{OL}(n)=239.7$ mb, also agrees with experiment [18] within quoted errors.

The structure of the ^{19}C ground state and the last neutron separation energy S_n are still very uncertain. A naive shell model suggests a nodeless $1d_{5/2}$ orbit for the least bound neutron. More detailed calculations however predict a $1/2^+$ ^{19}C ground state due to a lowering of the $2s_{1/2}$ orbital [19]. A $3/2^+$ or $5/2^+$ ground state remains a theoretical possibility [20], but would involve $(2^+\otimes 2s_{1/2})$ and/or $(2^+\otimes 1d_{5/2})$ excited ^{18}C core components, and $(2^+\otimes 2s_{1/2})$ and/or $(0^+\otimes 1d_{5/2})$ components, respectively. We consider both $2s_{1/2}$ and $1d_{5/2}$ neutron configurations (a) with separation energy $S_n=0.24\pm0.10$ MeV about a ^{18}C (0^+; g.s.) core, and (b) with separation energy $S_n=1.86\pm0.10$ MeV about a ^{18}C (2^+; 1.62 MeV) excited core. Very recently, a semiclassical analysis of new, kinematically complete, measurements of the Coulomb dissociation of ^{19}C, showed the data to be consistent with $S_n\approx0.50$ MeV [20,21]. We consider briefly the consistency of this proposal with the measured interaction cross sections. In [21] a spectroscopic factor of 0.67 for this more bound $(0^+\otimes 2s_{1/2})$ neutron configuration was also suggested, however the sensitivity of this extracted spectroscopic factor to the geometry of the assumed (Woods-Saxon) n+^{18}C binding potential was not clarified there.

Figure 1 shows the calculated reaction cross sections in the few-body (solid circles) and optical limit (open circles) approaches for ^{19}C+^{12}C at 960 MeV/nucleon. Following [15], we initially assume a Woods-Saxon n+^{18}C binding interaction with radius parameter $r_0=1.22$ fm, diffuseness $a=0.7$ fm, and neutron separation energies 0.24 ± 0.10 MeV and 1.86 ± 0.10 MeV for the core ground and excited state configurations, respectively. The horizontal lines show the experimental interaction cross section datum (solid line) and associated error bounds (dashed lines), $\sigma_I(^{19}\mathrm{C})=1231\pm28$ mb [15]. The calculated cross sections are shown for each of the possible ground state configurations discussed above. All calculations use a spectroscopic factor of unity. The error bar, visible on the $(0^+\otimes 2s_{1/2})$ FB calculation, is due to the assumed 100 keV error on S_n only. In all other configurations, the error from this source is smaller than the size of the points. The OL calculations, shown without errors, are consistent with those of [15] within quoted errors.

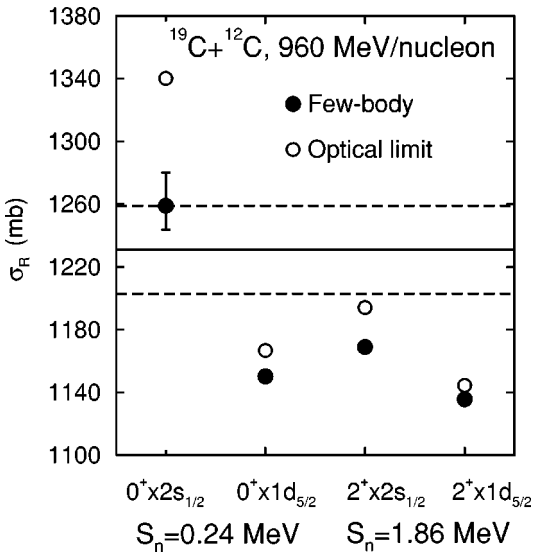

FIG. 1. Calculated reaction cross sections in the few-body model (solid symbols) and optical limit approximation (open symbols), for ^{19}C+^{12}C at 960 MeV/nucleon, for each of the possible neutron ground state configurations (see text).

Figure 1 shows that the calculated FB cross sections, particularly for the $2s_{1/2}$ configurations, are significantly smaller than those of the OL calculations. This is especially important for the $(0^+\otimes 2s_{1/2})$ neutron-halo configuration. This result is entirely anticipated for a single neutron halo system, e.g. [8], due to the increased transparency [9,11] of the collision in the case of the explicit FB treatment. Whereas the OL $(0^+\otimes 2s_{1/2})$ σ_R^{OL} lies outside the quoted error bar on σ_I by approximately 80 mb, the FB σ_R^{FB} overlaps the experimental error. In addition, the significant ($\approx$25 mb) suppression of the $(2^+\otimes 2s_{1/2})$ cross section would now appear to exclude both $J^\pi=3/2^+$ and $5/2^+$ as likely ground state configurations. This conclusion was also drawn from Coulomb dissociation data in [21]. Thus, based on a neutron binding interaction with geometry $(r_0,a)=(1.22,0.7)$, the FB calculations suggest that only a dominant $(0^+\otimes 2s_{1/2})$ neutron configuration, and hence a $J^\pi=1/2^+$ ^{19}C ground state, can reproduce the measured $\sigma_I(^{19}\mathrm{C})$. The calculated FB cross sections and measured σ_I are consistent with a spectroscopic factor of 0.80 ± 0.20 for the $(0^+\otimes 2s_{1/2})$ neutron configuration and therefore only a small $(2^+\otimes 1d_{5/2})$ admixture. This contrasts with the OL results, see also [15], using which the deduced spectroscopic factor of the halo state would be only

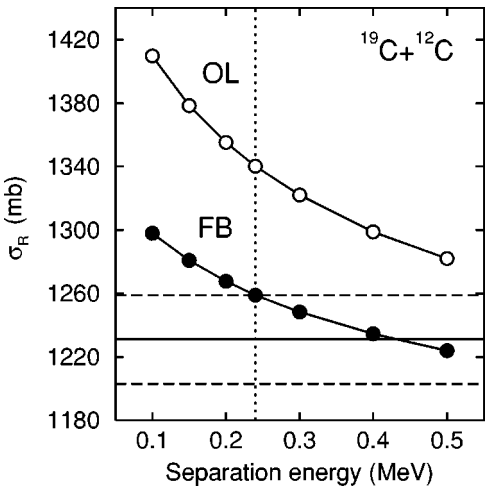

FIG. 2. Calculated reaction cross sections in the few-body model (solid symbols) and optical limit approximation (open symbols), for ^{19}C+^{12}C at 960 MeV/nucleon, for a $(0^+\otimes 2s_{1/2})$ neutron halo configuration, as a function of the assumed neutron separation energy S_n. The binding potential geometry is $(r_0,a)=(1.22, 0.7)$.

0.45 ± 0.18. The corresponding deduced ^{19}C rms radii $\langle r^2\rangle_{19}^{1/2}$ are also very different, 3.25 fm and 3.04 fm, in the FB and OL cases, respectively. These are seen to imply a significantly larger $\langle r^2\rangle_{19}^{1/2}-\langle r^2\rangle_{18}^{1/2}$ and halo extension in the FB case. The deduced rms neutron-core separations are 8.56 fm (FB) and 6.84 fm (OL) from the two calculations.

Given the empirical uncertainty in the last neutron separation energy S_n in ^{19}C, Fig. 2 shows the calculated FB and OL $\sigma_R(^{19}\mathrm{C})$ at 960 MeV/nucleon for the $(0^+\otimes 2s_{1/2})$ halo configuration as a function of the assumed S_n. The potential geometry $(r_0,a)=(1.22, 0.7)$ is assumed. The horizontal band shows the experimental interaction cross section datum and the vertical dotted line the values for $S_n=0.24$ MeV, as above. All calculations assume a spectroscopic factor of unity. The overestimate of $\sigma_R(^{19}\mathrm{C})$ in the OL calculations is again evident. Moreover, the figure shows the measured $\sigma_I(^{19}\mathrm{C})$ is entirely consistent, for this binding potential geometry, with $S_n\approx 0.5$ MeV and a spectroscopic factor of essentially unity. As seen above, reducing S_n increases the cross section which then requires a small $(2^+\otimes 1d_{5/2})$ admixture to fit the measured value.

Figure 3 shows the FB and OL $\sigma_R(^{19}\mathrm{C})$, but now as a function of the rms radius of the ^{19}C. As previously, the horizontal band shows the experimental interaction cross-section datum and all calculations use the potential geometry $(r_0,a)=(1.22, 0.7)$. The rms radii differ here by virtue of the differences in the assumed S_n, the value (in MeV) for each calculation being indicated in the lower part of the figure. Again the figure shows the $\sigma_I(^{19}\mathrm{C})$ datum to be consistent with a pure $(0^+\otimes 2s_{1/2})$ state of $S_n\approx 0.5$ MeV, in which case $\langle r^2\rangle_{19}^{1/2}\approx 3.1$ fm.

The calculations above have not considered the cross-section sensitivity to the assumed neutron binding potential geometry (r_0,a). Figure 4 shows the calculated FB and OL $\sigma_R(^{19}\mathrm{C})$ as a function of the ^{19}C rms matter radius, but now for a set of wave functions with a fixed $S_n=0.24$ MeV. The solid lines connect calculations which assume $(0^+\otimes 2s_{1/2})$ wave functions from well geometries $(1.22,a)$ with different

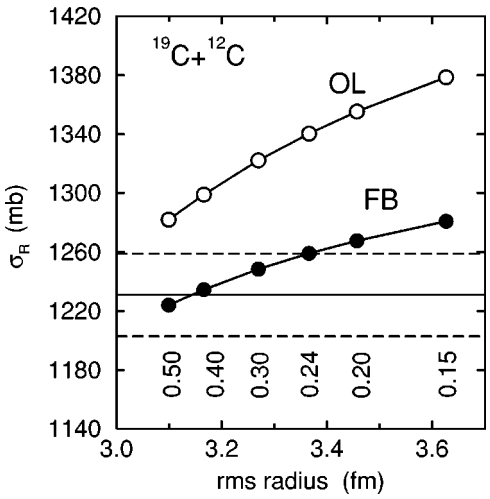

FIG. 3. Calculated reaction cross sections in the few-body model (solid symbols) and optical limit approximation (open symbols), for ^{19}C+^{12}C at 960 MeV/nucleon, as a function of the rms radius of ^{19}C. The binding potential geometry is $(r_0,a)=(1.22, 0.7)$, and the single neutron separation energies S_n (in MeV) used in each case are indicated.

a. The well depths were adjusted to reproduce S_n. The calculations run from $a=0.2$ fm for the left-most points to $a=1.0$ fm for the extreme right hand point in steps of 0.1 fm. We note that the $\sigma_I(^{19}\mathrm{C})$ datum can be reproduced by a pure $(0^+\otimes 2s_{1/2})$ state of $S_n=0.24$ MeV, but through the use of what are probably unphysically small diffuseness parameters (or radius parameters, not shown here). The use of more usual shell model parameters requires the small $(2^+\otimes 1d_{5/2})$ admixture observed earlier, although the errors on the measurement make more quantitative discussions difficult. Figure 5 shows similar calculations, but now assuming $S_n=0.50$ MeV. We note only that the measured $\sigma_I(^{19}\mathrm{C})$ is entirely consistent with a $(0^+\otimes 2s_{1/2})$ halo state of $S_n=0.50$ MeV for a wide range of physically reasonable effec-

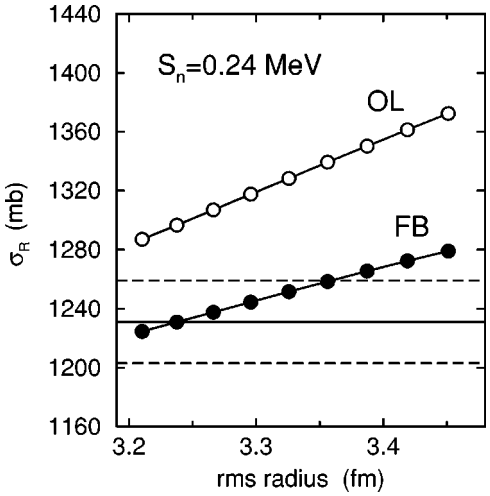

FIG. 4. Calculated reaction cross sections in the few-body model (solid symbols) and optical limit approximation (open symbols), for ^{19}C+^{12}C at 960 MeV/nucleon, as a function of the rms radius of the ^{19}C. The binding potential radius is $r_0=1.22$ fm and the diffuseness a has been varied to obtain states with different rms radii. The neutron separation energy is 0.24 MeV in all cases.

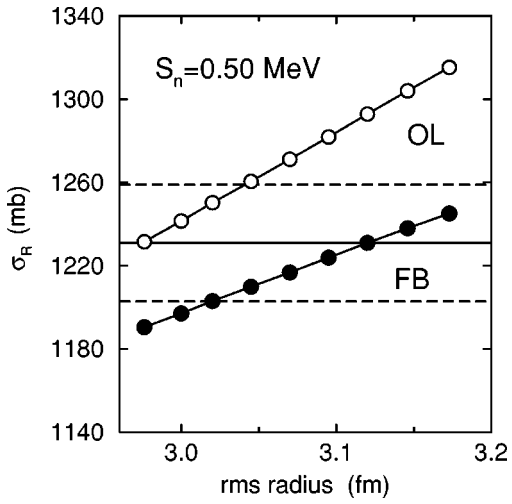

FIG. 5. As for Fig. 4, but for a neutron separation energy of 0.50 MeV.

tive binding potential geometries.

We have calculated reaction cross sections for the ^{19}C+^{12}C system at relativistic energies within the FB framework. As was observed in earlier work for one- and two-neutron halo nuclei, there is increased transparency in the collision compared to calculations which use the OL approximation to Glauber theory, an approximation which is inappropriate for loosely bound few-body structures. The calculated FB cross sections are significantly smaller than those of the OL approximation, particularly for the possible $2s_{1/2}$ neutron configurations in the ^{19}C ground state. These reduced cross sections change markedly the deduced $(0^+ \otimes 2s_{1/2})$ spectroscopic factor in the ^{19}C ground state and also the deduced difference in rms size of the ^{18}C and ^{19}C isotopes from the measured interaction cross sections.

We show that in the FB picture, for reasonable neutron+^{18}C binding potential geometries, the measured ^{19}C interaction cross section is consistent with a $J^\pi = 1/2^+$ ^{19}C ground state with $S_n = 0.24$ MeV and with a dominant $(0^+ \otimes 2s_{1/2})$ neutron configuration with spectroscopic factor of order 0.80 ± 0.20. The FB calculations exclude $J^\pi = 3/2^+$ and $5/2^+$ ground states as likely configurations. The datum is also however consistent with a pure $(0^+ \otimes 2s_{1/2})$ state having a separation energy $S_n \approx 0.5$ MeV. In combination with independent experimental data, such as from Coulomb dissociation measurements and from momentum distributions following ^{19}C breakup reactions, the interaction cross section measurement may thus provide a useful constraint on the ^{19}C ground state. Such a measurement with even higher precision could prove to be very powerful.

ACKNOWLEDGMENTS

The financial support of the United Kingdom Engineering and Physical Sciences Research Council (EPSRC) in the form of Grant No. GR/J95867 is gratefully acknowledged.

[1] I. Tanihata *et al.*, Phys. Rev. Lett. **55**, 2676 (1985).
[2] I. Tanihata *et al.*, Phys. Lett. B **160**, 380 (1985).
[3] I. Tanihata, T. Kobayashi, O. Yamakawa, S. Shimoura, K. Ekuni, K. Sugimoto, N. Takahashi, T. Shimoda, and H. Sato, Phys. Lett. B **206**, 592 (1988).
[4] R. J. Glauber, in *Lectures in Theoretical Physics*, edited by W. E. Brittin (Interscience, N.Y., 1959), Vol. 1, p. 315.
[5] W. Czyz and L. C. Maximon, Ann. Phys. (N.Y.) **52**, 59 (1969).
[6] P. J. Karol, Phys. Rev. C **11**, 1203 (1974).
[7] S. Kox *et al.*, Phys. Rev. C **35**, 1678 (1987).
[8] J. S. Al-Khalili and J. A. Tostevin, Phys. Rev. Lett. **76**, 3903 (1996).
[9] J. S. Al-Khalili, J. A. Tostevin, and I. J. Thompson, Phys. Rev. C **54**, 1843 (1996).
[10] J. A. Tostevin and J. S. Al-Khalili, Nucl. Phys. **A616**, 418c (1997).
[11] J. A. Tostevin, R. C. Johnson, and J. S. Al-Khalili, Nucl. Phys. **A630**, 340c (1998).
[12] D. Bazin *et al.*, Phys. Rev. Lett. **74**, 3569 (1995).
[13] F. M. Marqués *et al.*, Phys. Lett. B **381**, 407 (1996).
[14] N. A. Orr *et al.*, Phys. Lett. B **258**, 29 (1991), and references therein.
[15] A. Ozawa *et al.*, *Measurements of interaction cross sections for Carbon isotopes at relativistic energies and the halo structure of ^{19}C*, RIKEN Report No. RIKEN-AF-NP-294, 1998, Phys. Rev. Lett. (submitted).
[16] Y. Ogawa, K. Yabana, and Y. Suzuki, Nucl. Phys. **A543**, 722 (1992).
[17] S. K. Charagi and S. K. Gupta, Phys. Rev. C **41**, 1610 (1990).
[18] W. Bauhoff, At. Data Nucl. Data Tables **35**, 429 (1986).
[19] E. K. Warburton and B. A. Brown, Phys. Rev. C **46**, 923 (1992).
[20] D. Ridikas, M. H. Smedberg, J. S. Vaagen, and M. V. Zhukov, Europhys. Lett. **37**, 385 (1997); Nucl. Phys. **A628**, 363 (1998).
[21] T. Nakamura *et al.*, *Coulomb dissociation of ^{19}C*, in Proceedings of the 2nd International Conference on Exotic Nuclei and Atomic Masses (ENAM98), edited by B. M Sherrill, D. J. Morrissey, and C. N. Davids, AIP Conf. No. 455 (AIP, New York, 1998).